Article

Effect of Delivery Platforms Structure on the Epidermal Antigen Transport for Topical Vaccination

Ana S. Sonzogni, Guy Yealland, Mrityunjoy Kar, Stefanie Wedepohl, Luis M. Gugliotta, Verónica D.G. Gonzalez, Sarah Hedtrich, Marcelo Calderon, and Roque J. Minari

Biomacromolecules, **Just Accepted Manuscript** • DOI: 10.1021/acs.biomac.8b01307 • Publication Date (Web): 30 Oct 2018

Effect of Delivery Platforms Structure on the Epidermal Antigen Transport for Topical Vaccination

Ana S. Sonzogni[1], Guy Yealland[2], Mrityunjoy Kar[3], Stefanie Wedepohl[3], Luis M. Gugliotta[1], Verónica D.G. Gonzalez[1], Sarah Hedtrich[2], Marcelo Calderón[3#], Roque J. Minari1[*]

1 Group of Polymers and Polymerization Reactors, INTEC (Universidad Nacional del Litoral-CONICET), Güemes 3450, Santa Fe 3000, Argentina.

2 Freie Universität Berlin, Institute of Pharmacy, Königin-Luise-Str. 2+4, 14195 Berlin, Germany

3 Freie Universität Berlin, Institute of Chemistry and Biochemistry, Takustrasse 3, 14195 Berlin, Germany

Corresponding Authors

*E-mail: rjminari@santafe-conicet.gov.ar

E-mail: marcelo.calderon@fu-berlin.de

ABSTRACT. Transdermal immunization is highly attractive owing to the skin accessibility and unique immunological character. However, it remains a relatively unexplored route of administration owing to the great difficulty of transporting antigens past the outermost layer of skin, the stratum corneum. In this article, the abilities of three poly(*N*-vinylcaprolactam) (PVCL) based thermoresponsive assemblies – PVCL hydrogels and nanogels plus novel film forming PVCL/acrylic nanogels – to act as protein delivery systems were investigated. Similar thermal responses were observed in all systems, with transition temperatures close to 32 °C, close to that of the skin surface. The investigated dermal delivery systems showed no evidence of cytotoxicity in human fibroblasts and were able to load and release ovalbumin (OVA), a well-studied antigen, in a temperature dependent manner *in vitro*. The penetration of OVA into *ex vivo* human skin following topical application was evaluated, where enhanced skin delivery was seen for the OVA loaded PVCL systems relative to administration of the protein alone. The distinct protein release and skin penetration profiles observed for the different PVCL assemblies were here discussed on the basis of their structural differences.

KEYWORDS. poly(N-vinylcaprolaptam), thermoresponsive polymers, dermal delivery systems, protein skin penetration, transdermal immunization

INTRODUCTION

The skin is the primary barrier of the body against invading pathogens.1 For this reason, a large population of immunocompetent cells such as keratinocytes, Langerhans cells, subsets of T lymphocytes, and skin-associated lymphoid tissue are found within the epidermis and dermis.[2] Langerhans cells are professional antigen-presenting cells that induce antigen-specific T cell adaptive immuneresponses.3 Thus, efficient antigen delivery to epidermal Langerhans cells could generate specific immune responses[4]. However, the stratum corneum (SC), the outermost layer of skin, is a highly efficient barrier that few molecules are known to passively traverse. Key factors to SC penetration include small molecular weight (< 500 Da) and moderate lipophilicity.[5,6] Although the idea of transdermal vaccination is gaining prominence,[7–11] its realization will require effective and reproducible penetration of large molecules past the SC and into the skin.

Chemical and biological penetration enhancers, as well as semi-invasive techniques that physically disrupt the ordering of the SC, have been proposed as methods to facilitate the skin penetration of large macromolecules.[12–18] Among these strategies, the use of hydrogels – crosslinked polymer networks capable of absorbing large amounts of water or biological fluids – has been shown to enhance the topical delivery of bovine serum albumin into barrier intact skin as well as barrier deficient skin, a condition found in many skin diseases.[19] Hydrogel patch formulations have been used to effectively induce

immune responses to tetanus and diphtheria toxins in hairless rats.[20] Evidences obtained from these studies indicate that the enhancement to topical antigen delivery results from the skin hydration effect of hydrogel application in addition to their disrupting interactions with SC components. Similarly, several thermoresponsive nanogels (NGs, hydrogels of nanometric size) have been shown to encapsulate a range of proteins (with molecular weight as high as ~150 kDa) and mediate their penetration past the SC of barrier deficient human skin. It is believed that penetration through the SC is facilitated by the triggered release of protein after the topical application, and interactions between the NGs and the SC.[21–24]

Recently, a successful strategy for synthesizing thermosensitive PVCL based NGs with film-forming ability was developed.[25] These resulting NGs (PVCL/acrylic NGs) presented two clearly distinguished phases: crosslinked PVCL and soft acrylic copolymer with a low glass transition temperature (Tg). The low Tg of acrylic phase allowed for the coalescence of the NGs and the formation of nanostructured and flexible PVCL/acrylic patches. In the current work, the performance of the PVCL/acrylic patch as a topical protein delivery system was investigated and compared to pure PVCL hydrogels and NGs. Although extensive information regarding NGs and hydrogels is available in literature, this paper exclusively compares the performance of these different crosslinked PVCL materials and their abilities as platforms for the topical delivery of proteins (Figure 1.a). PVCL was chosen as the base polymer for the three

considered systems owing to its biocompatibility[26] and thermoresponsive properties.[27] Owing to the thermoresponsive character of PVCL, the investigated systems exist in one of two states. Below their transition temperature, the PVCL is soluble and so the hydrogel networks expand and swell with water. Above their transition temperature, the PVCL becomes insoluble causing any previously hosted fluid to be expelled from the hydrogel (Figure 1.b). Synthesis parameters were chosen to fine tune the transition temperature between these two states to be near the skin surface temperature, 32 °C. It is hoped that the PVCL/acrylic NGs will offer improved skin penetration properties by combining the high loading capacity of a NG with the occlussive effect generated by topical application of a patch.[25] Ovalbumin (OVA), one of the most popular antigen models, was chosen as model protein for this study. The three systems transition temperatures and cytotoxicity, as well as their OVA loading capacities, in vitro release profiles and skin penetration abilities were evaluated in order to determine the effect of their structural composition on the epidermal transport of antigens.

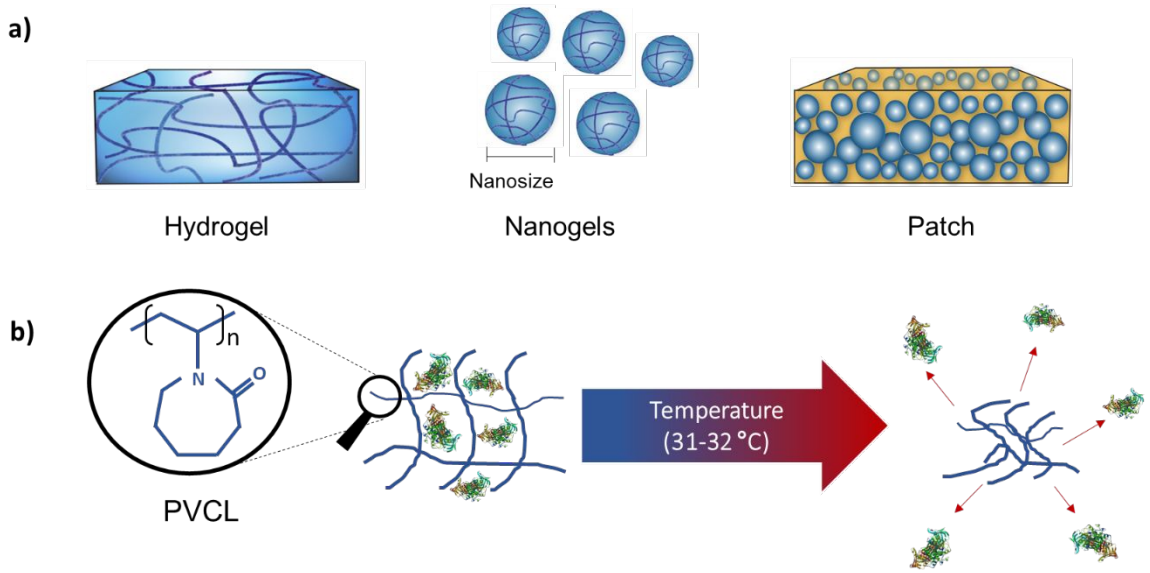

Figure 1. Scheme of (a) the three investigated systems and of the thermoresponsive character of PVCL (b).

MATERIALS

N-vinylcaprolactam (VCL, 98% purity, Aldrich), butyl acrylate (BA, 99% purity, Aldrich), and acrylic acid (AA, 98% purity, Aldrich), were used as monomers and *N,N*-methylenebisacrylamide (BIS, 99.9% purity, Genbiotech) as crosslinking agent. Potassium persulfate (KPS, 99% purity, Mallinckrodt), and 2,2'-Azobis(2-methylpropionitrile) (AIBN, 98% purity, Aldrich) were used as initiators (I). Other reagents were: sodium bicarbonate ($NaHCO_3$, 99.7% purity, Cicarelli) as buffer, sodium dodecyl sulphate (SDS, Anedra) as emulsifier, and hydroquinone as polymerization inhibitor (99% purity, Fluka AG). All the above reagents were employed as received without purification. Ovalbumin from chicken egg (OVA, 98% purity, Aldrich) was

used as model protein. *Ex vivo* skin penetration experiments were conducted in a transwell system (5 μm pore size, Corning) and assessed by immunofluorescence of cryo-embedded sections (Surgipath FSC22 embedding-media, Leica Biosystems) using antibodies against OVA and rabbit IgG (ab181688 and ab150080 respectively, Abcam) and 4',6-diamidin-2-phenylindol (DAPI) antifading mounting medium (Dianova). Distilled and deionized water was used throughout the work.

METHODS

Synthesis of delivery systems

Polymerization temperature for all synthetic procedures experiments was 70 °C. In all polymerizations, a ratio BIS/VCL of 4% was adopted, in order to obtain a similar transition temperature in the three systems. While the hydrogel was synthesized in a syringe, NG syntheses were carried out in a 200 mL jacketed glass reactor equipped with an automatic feeding system, mechanical stirring, steam condenser, sampling output, nitrogen inlet, digital thermometer, and a thermostatic bath.

PVCL/acrylic Patches

The PVCL/acrylic patches were prepared in two steps. The first one involved the synthesis of PVCL/acrylic NGs and their purification. Then, in a second step the patch was obtained by casting the PVCL/acrylic NG dispersion.

PVCL/acrylic NGs were synthesized following the previously reported semibatch procedure.[25] This involves loading 50% of the formulation corresponding to water into the reactor in batch, VCL, SDS, $NaHCO_3$, and the whole amount of BIS. After reaching

the reaction temperature and purging the dispersion with N_2 for 60 min, a KPS solution was injected to initiate the polymerization. The remaining 50% of water, VCL, SDS, $NaHCO_3$ was fed at a constant feed rate during 90 min from the beginning of the reaction. After 50 min of polymerization, an aqueous dispersion containing the acrylic monomers (BA and AA), was fed at a constant feed rate during 40 min. Once the feeding period was finished, polymerization conditions were maintained for additional 30 min. Then, the synthesized NGs were purified by dialysis against distilled and deionized water, to remove the unreacted monomers, the emulsifier and impurities. The final content of dialyzed PVCL/acrylic NGs dispersion, 54.5 mg/mL, was gravimetrically determined onto a small aliquot before patches formation.

Patches were prepared by casting the dialyzed NGs dispersion containing 22 mg of PVCL/acrylic NGs onto moulds of 10 mm of diameter and drying at room temperature in a desiccator with silica gel until achieving a constant weight. The final PVCL/acrylic patch thickness was about 1 mm.

PVCL Nanogels

Unlike the semibatch synthesis procedure employed for obtaining PVCL/acrylic NGs, PVCL NGs were prepared in batch as follows. VCL, BIS, $NaHCO_3$, SDS and water were loaded into the reactor, and kept under stirring and nitrogen bubbling at the reaction temperature for 60 min. Then KPS, predissolved in a small amount of water, was injected into the reactor to initiate the polymerization. Reaction conditions were

maintained during 120 min. The obtained NGs dispersions were purified by dialysis. Finally, dialysed PVCL NGs were lyophilized.

Hydrogels

VCL, BIS and AIBN were dissolved in an ethanol-water mixture (70-30) and the reaction mixture was loaded into 3 mL syringes (10 mm diameter). Nitrogen was bubbled for 15 minutes and the syringe was immersed in an ultrasonic bath, for 5 min, to remove any bubbles present. The system was kept for 4 h at the reaction temperature. The obtained gel bar was cut with a scalpel in cylinders of similar height and washed repeatedly in deionized water to remove the polymerization residues.

Characterization

Morphology

Morphology of synthesized systems was characterized by electron microscopy. The patch and the hydrogel were freeze-dried and the first one was then gold-coated using a sputtering Emitech model K500X, with a voltage of 2 kV and for 3 min. Samples of patch and hydrogel were observed using a Phenom World ProX scanning electron microscopy (SEM). PVCL NGs were observed with transmission electron microscopy (TEM) with a Hitachi Scanning Electron Microscope (SU8030). Samples were prepared by depositing a diluited NG dispersion with a concentration of 1 mg/ml on copper grids, and drying at room temperature.

Thermal response analysis

The thermal response of all of the investigated materials was evaluated in water. The thermal response of the patch and hydrogel was determined by immersing a sample in deionized water at different temperatures (20, 30, 35, 40, 50 and 55 ºC). At each temperature, samples were maintained one hour to reach the equilibrium and the absorbed water was determined gravimetrically, by removing the sample from the medium, drying with paper filter, and immediately weighting before immersing again. This procedure was repeated per triplicate.

The thermal response of NGs was determined by measuring the average particles diameter (*D*) of dilute samples (1 mg/mL) at increasing temperatures (from 20 ºC up to 55 ºC at intervals of 2.5 ºC, with 20 min of stabilization). *D* was measured by dynamic light scattering (DLS) at a detection angle of 90º, in a Brookhaven BI-9000 AT photometer.

Swelling factor parameter based on weight ($Ø_w$) and on volume ($Ø_v$) was defined in order to compare transition temperature of the three systems, according to Eq. 1 for patch and hydrogel, and to Eq. 2 for NGs.

$$\emptyset_w(T) = 1 - \frac{W_S - W(T)}{W_S - W_C} \qquad \textbf{(Eq. 1)}$$

$$\emptyset_v(T) = 1 - \frac{V_S - V(T)}{V_S - V_C} \qquad \textbf{(Eq. 2)}$$

Where W_S and V_S are the weight and the volume at the swelling state (20 °C), W_C and V_C are the weight and the volume at the collapse state (55 °C), and $W(T)$ and $V(T)$

are the weight and the volume at the measured temperature (T). It can be seen that in the swelling state $Ø_I(T) = 1$ for both definitions, and in the collapsed state $Ø_I(T) = 0$.

Cell viability assay

The cytotoxicity of each material was evaluated by measuring the adenosine triphosphate (ATP) content of human dermal fibroblasts after 48 h exposure to dispersions of PVCL NGs and PVCL/acrylic NGs and to an extract of the hydrogel, using CellTiter-Glo® luminescent cell viability assay (Promega). To obtain the hydrogel extracts, the sample was incubated in 1 mL of cell growth medium [DMEM with 10% fetal bovine serum (FBS) and 1% penicillin/streptomycin (P/S)] for 48 h at 37 °C. Fibroblasts were seeded into white flat 96-well plates at a density of 10^5 cells/mL in 100 µL/well and grown over night at 37 °C and 5% CO_2. The next day, the supernatant was removed and replaced with 100 µL/well of the hydrogel extracts (100% medium replacement) or diluted to 10%, 1%, 0.1% and 0.01% in fresh medium and incubated for another 48 h. Cells incubated with fresh medium only served as a control. For the study of NGs dispersions, cells were seeded at a density of 10^5 cells/mL into white flat 96-well plates at 100 µL/well and incubated overnight at 37 °C and 5% of CO_2. The next day, the NGs were added in 10-fold serial dilution in medium starting from 5 mg/mL as a maximum, in duplicates. For all experiments, three independent plates were prepared. After each incubation, CellTiter-Glo assay was performed according to the instructions of the manufacturer. Luminescence was read in a Tecan Infinite M200Pro microplate

reader. The relative viability was calculated by dividing luminescence values of treated cells by values of untreated cells.

OVA loading in the carrier systems

Loading of film patch involves first the dissolution of 3 mg of OVA in 0.4 mL of the PVCL/acrylic NGs dispersion (containing 22 mg of NGs). Then, OVA loaded film patch was obtained by casting the previous dispersion into silicone moulds and drying at room temperature in a desiccator with silica gel until a constant weight.

OVA loading into the hydrogel was carried out by immersing a dry sample in a solution of OVA of 17 mg/mL at 4 °C for 48 h. Then, the loaded hydrogel was removed. The concentration of OVA in the solution before the hydrogel immersion and after the hydrogel removal, was measured by UV/Vis spectroscopy. The absorbance at 280 nm was used to calculate the loaded OVA from the difference between both respective concentrations.

A similar procedure was followed to load the NGs. An OVA loaded PVCL NGs dispersion (with a final NGs content of 5 mg/mL) was prepared by redispersing the required mass of lyophilized NGs in an OVA solution of 4 mg/mL, and incubated during 48 h at 4 °C. After the incubation period, the suspension was filtered with a VIVASPIN centrifugal filter (molecular weight cut-off, MWCO, 300,000 Da) at 8000 rpm and for 15 min to separate the loaded NGs from the unloaded protein solution. The loaded OVA was determined following the procedure described for the hydrogel.

The loading capacity (LC) and encapsulation efficiency (EE, %) of the materials were calculated as follows.

$$LC = \frac{mass\ of\ OVA\ loaded}{mass\ of\ polymer\ carrier} \quad \textbf{Eq. 3}$$

$$EE = \frac{mass\ of\ OVA\ loaded}{mass\ of\ OVA\ added} \times 100 \quad \textbf{Eq. 4}$$

OVA release

OVA release study was performed using patch (22 mg), hydrogel (33 mg) and PVCL NGs dispersion (1 mL with a NGs concentration of 5 mg/mL) loaded with 3, 3.7, and 3.8 mg of OVA, respectively. The materials were incubated in PBS (pH = 7.4) at 25 and 37 °C for one week, per triplicate. At regular intervals, the release medium was replaced, and the amount of released protein was measured by Bradford assay.[28]

The secondary structure of the OVA released was determined by circular dichroism (CD) with a Jasco J-810 spectropolarimeter (Jasco, Gross-Umstadt, Germany) using a 0.2 mm path length Quartz Suprasil cuvettes (Hellma, Müllheim, Germany).

OVA skin penetration assay

Punch skin biopsies (20 mm diameter) were sectioned from ex vivo human skin, obtained from routine plastic surgeries with written and ethical consent (EA1/081/13). Sections were taken from either unaltered regions of skin, or areas previously subjected to tape stripping (50 times). These were then placed into transwell inserts held in 6 well

plates, and surrounded by 2 mL phosphate buffered saline (PBS). OVA loaded patches (22 mg polymer, 0.125 mg OVA), hydrogels (33 mg polymer, 0.125 mg OVA), and 525 μg/cm^2 of OVA loaded NG (0.4 mg polymer, 0.125 mg OVA) were applied to the surface of skin punches. These were then transferred to an incubator for 6 h and exposed to a temperature ramp (30 °C 0–1 h, 34 °C 1–2h, and 37 °C 2–6 h). Subsequently, excessive formulation was removed, and subsequently flash frozen. Afterwards, the skin was sectioned into 8 μm thick cross-sections (Leica CM1510, Leica Biosystems) fixed (paraformaldehyde, 4%) and immuno-stained against OVA (anti-OVA ab181688; Alexa-594 labelled anti-rabbit IgG ab150080, Abcam) according to routine procedures. The sections were then counterstained with DAPI and imaged by fluorescence microscopy (BZ-8000Keyence, Neu-Isenburg, Germany; objectives 20x/0.75, zoom 20x, Plan-Apo, DIC N2). Images were analysed using FIJI image analysis software, an ImageJ distribution.[29]

RESULTS AND DISCUSSION

After synthesizing the three investigated platforms, the monomer conversion, determined by NMR[25], was almost completed. Then, both synthesized NGs were purified by dialyzed against deionized water, while hydrogel was washed repeatedly in deionized water. Characterizations were carried out onto the purified systems. Smooth and flexible PVCL/acrylic patches were obtained by casting a room temperature the purified PVCL/acrylic NGs dispersion.

Structure of PVCL based carrier systems

The structural composition of the three investigated systems was evaluated in order to determine their effect on the epidermal transport of proteins (Figure 2). The hydrogel exhibited a crosslinked structure with a pore size in the range of 15-30 μm (Figure 2a). As expected, NG pores were naturally not visible by TEM, although their spherical morphology and a relatively narrow size distribution can be noted (Figure 2b). The SEM image of the patch shows a complete coalesced film with small pores at the surface that do not exceed 2 μm in diameter; it provides evidence of the good film-forming ability of PVCL/acrylic NGs (Figure 2c).

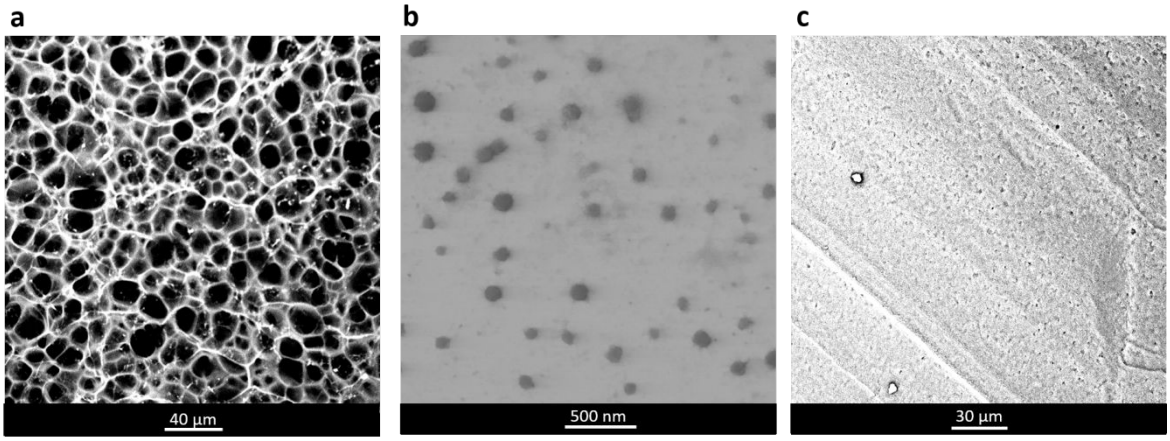

Figure 2. Microscopy images of the studied carrier platforms: (a) hydrogel, (b) PVCL NGs and (c) PVCL/acrylic patch.

The investigated systems notably differed in their exposed surface areas. The small size of NGs at 37 °C – 157 and 393 nm diameters for PVCL and PVCL/acrylic NGs, respectively – and therefore large surface area-to-volume-ratios, is advantageous for the mass transfer of protein during loading and release processes. On the other hand, a large

surface area exposed to the environment promotes a fast water evaporation, which could lead to an incomplete protein release on long-term applications, something less significant in larger hydrogels. Furthermore, patches are known to enhance skin penetration due to an increased hydration of the SC caused by occlusive effects.[30] In these contexts, the nanostructured patch obtained from coalesced PVCL/acrylic NGs is hoped to combine the advantages of both hydrogels and PVCL NGs.

Thermoresponsiveness of the PVCL carrier system

PVCL is a well-studied temperature-responsive polymer that exhibits classic Flory–Huggins thermoresponsive phase behavior in water (Type I)[31], where its lower critical solution temperature (LCST) increases with decreasing polymer chain length and concentration.[32] Below its LCST, the PVCL is soluble in water. Above this temperature, the polymers undergo a phase transition and collapse causing the PVCL to become insoluble. This phenomenon is reversible; when the temperature is lowered, the polymers become soluble again.[33,34] The PVCL is crosslinked within our three carrier systems, and the resulting three-dimensional structures undergo reversible volume changes between swollen and collapsed states. The presence of both states in all the three systems was confirmed by determination of their swelling factors – calculated from volume and weight changes ($Ø_v$ and $Ø_w$ respectively) – as a function of temperature (Figure 3a). The definition $Ø_i$ allows one to compare the thermal response of systems following different parameters: volume of the NGs and weight of the patch

and hydrogel. For the three systems a $Ø_i(T) = 1$ refers to the swollen state and a $Ø_i(T) = 0$ to collapsed state. The transition temperatures can be defined as the temperature when $Ø_i(T) = 0.5$ (Table 1).

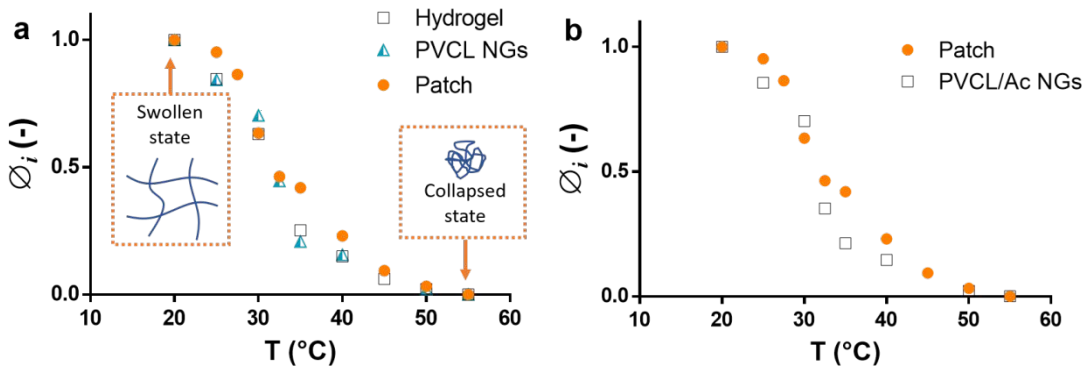

Figure 3. (a) Thermal response (in term of $Ø_w$ and $Ø_v$) of hydrogel, PVCL NGs and PVCL/acrylic patch. (b) Thermal response of patch and PVCL/acrylic NGs.

Table 1 –Transition temperatures (Øi(T) = 0.5) and percentage of water gain at 20 °C.

	Transition temperature	% water gain
Hydrogel	31.7	520 ± 10
PVCL NGs	31.4	1887 ± 2
PVCL/acrylicNGs	32.0	2079 ± 30
PVCL/acrylic Patch	32.0	446 ± 13

Parameters determine by volume changes for NGs and weight changes for patch and hydrogel.

All investigated systems presented broad thermal transitions almost covering the entire investigated temperature range (25 to 45 °C) (Figure 3), and corresponding to the phase separation of PVCL at its LCST,[35] with the transition temperatures in all cases

between 31 and 32 °C. The reason for the wide range of transition could relate to the broad MW distribution of PVCL inside the gel structures; taking into account that the LCST of the PVCL varies with molecular weight. The different chain lengths present in systems likely produce progressive contraction with increasing temperature. This behavior could also be observed in previous studies of PVCL based NGs, where wider ranges of transitions were obtained by augmenting the crosslinker and emulsifier content.[36]

Although the carrier systems have different structures and morphologies (Figure 2), they allow to hold great amounts of water as well as water soluble drugs or macromolecules, retaining them until the time of release. Indeed, skin hydration is the most widely and safest used method to increase skin penetration of both hydrophilic[37] and lipophilic[38] molecules. Thus, the application of our systems and their high water contents could also function as a penetration enhancer through the hydration of the SC.

Water gain percentage between collapsed and swollen states was determined by measuring the weight gain of the hydrogel and patch, and volume gain of the NGs (Table 1). The water gain percentage of the PVCL/acrylic NGs dispersion was similar to that of pure PVCL NGs. In agreement, DLS measurement revealed similar levels of contractility between the two systems, with average diameter (*D*) variations of 100 nm and 169 nm between room 25 °C and 37 °C for PVCL and PVCL/acrylic NGs, respectively (Figure 4). Notably, both NG dispersions showed narrow, monomodal size

distribution (in intensity and in volume with relatively low polydispersity index/PDI). The water gain in the patch formed from coalesced PVCL/acrylic NGs was similar to that of the hydrogel (around 4 times less than the NGs dispersions), indicating a close swelling capacity for both macro-systems. It was also noted that the transition temperature was practically the same for both of PVCL/acrylic NGs and the obtained patch, indicating that the film formation process does not interfere with this property (Figure 3b and Table 1). Remarkably, the transition temperatures of the three systems were all appropriate for skin delivery applications, since skin temperature is 32 °C at the surface and rises with increasing depth.[39]

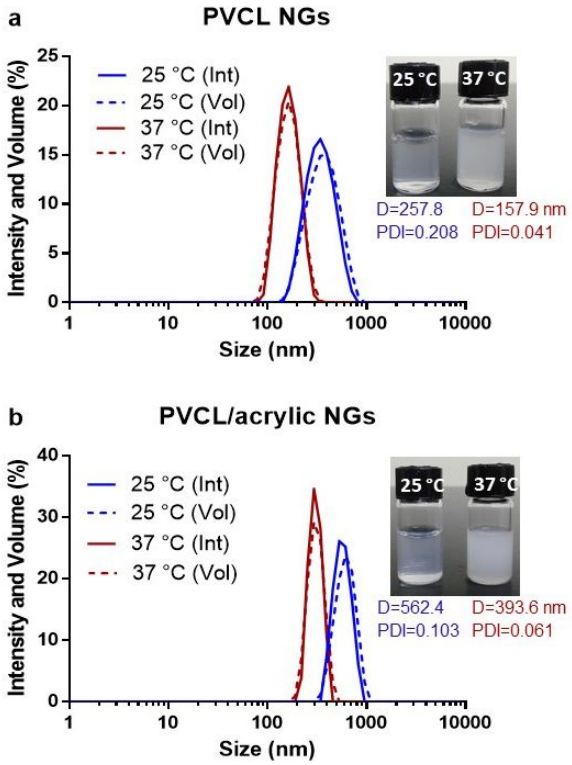

Figure 4. DLS intensity and volume distributions at 25 and 37 °C of (a) PVCL NGs and (b) PVCL/acrylic NGs.

Carrier system biocompatibility

PVCL is, reportedly, better tolerated by cells than many other thermoresponsive polymers.[26] Although all three systems are based on PVCL, the presence of surface charge, acrylic comonomers in the PVCL/acrylic NGs, and possible remnants from the synthetic process (e.g. monomers and emulsifier) even after the washing process, could interfere with this property. In this context, the cytotoxicity of the three delivery systems was evaluated in human dermal fibroblasts. As shown in Figure 5a, 97% of cell viability was retained when the media was replaced with 100% of hydrogel extract. Similarly, cell viabilities of 99% and 84% following incubation with PVCL and PVCL/acrylic NGs (5 mg/mL) respectively were obtained (Figure 5b). One possible reason for the slightly decreased cell viability following PVCL/acrylic NG treatment is the presence of a large amount of negative charged acrylic acid[40]. These results confirmed that all the three materials were well tolerated by human dermal fibroblasts, with all showing greater than 75% cell viability at the highest tested concentration.

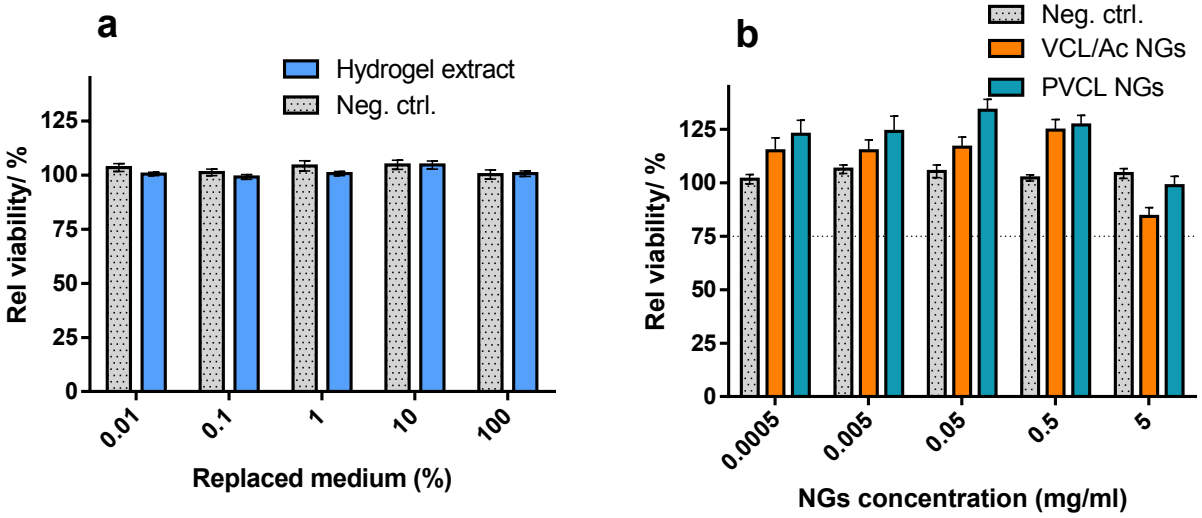

Figure 5. Relative viabilities of human dermal fibroblast after 48 h of exposure to (a) hydrogel extract and (b) different concentrations of PVCL and PVCL/acrylic NGs (n=3, mean ± SD).

OVA loading and thermally triggered release

The OVA loading capacities (LC; Eq. 3) and encapsulation efficiencies (EE; Eq. 4) of the three systems were quantified (Figure 6). Differences between the loading processes of each system must be considered when interpreting these results. For the PVCL NGs and hydrogels, unencapsulated OVA was separated from the obtained delivering carrier materials, and therefore they contain only the encapsulated protein. For the case of OVA loaded in the PVCL/acrylic patch, the total mass of protein added to the NG dispersion was available in the final patch.

As expected, PVCL NGs possessed the highest LC value, encapsulating almost all of added OVA (EE = 94 %). Because PVCL NGs have the largest surface area to volume

ratio, their LC value was those for higher than the other two systems. PVCL/acrylic NGs presented an EE of 60 %, lower than that obtained for pure PVCL NGs. This may result from the acrylic phase of PVCL/acrylic NGs does not contribute to OVA encapsulation. Despite this, the PVCL/acrylic patch demonstrated an EE 100%, likely due to the specific method used to load OVA in this system. Here, the protein was incubated with the PVCL/acrylic NGs dispersion, which was then used to cast the patch without separation of the non-encapsulated OVA. Therefore, all the loaded protein remained in the patch after water evaporation, where a fraction of OVA was encapsulated inside the PVCL/acrylic NGs structure and the rest of it could remain in the interstitial spaces among the NGs particles in the film. Patch formation process could change the distribution of OVA within it since this involves the evaporation of water both as, primarily, a disperse media and fraction within the swollen NG structures. It is expected that the freely dispersed water evaporates more easily than entrapped in NG interiors. This difference in water evaporation rate could promote the migration of OVA soluble in the free water toward NG structures.

The PVCL hydrogel presented the lowest EE, likely due to this system exhibited lower surface-area-to-volume-ratio. The final obtained OVA concentration per mass polymer (LC) was, however, similar to that observed for the other macro-carrier, the PVCL/acrylic patch.

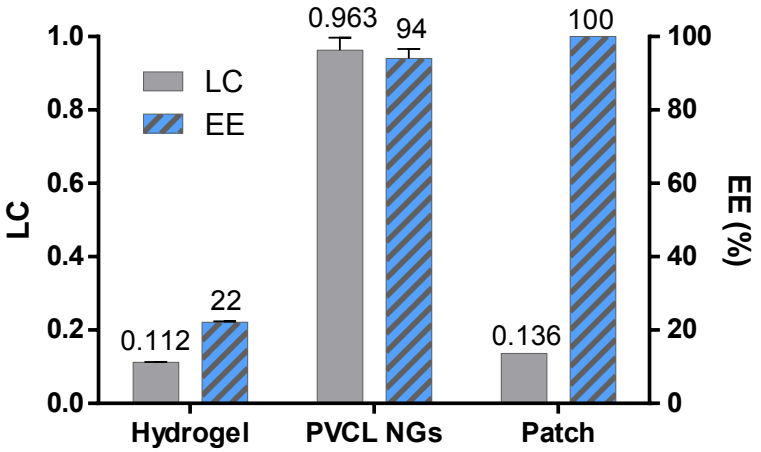

Figure 6. OVA loading capacity (LC) and encapsulation efficiency (EE) of the systems (n=3, mean ± SD).

The release profile of OVA from all three carrier systems at 25 and 37 °C was determined (Figure 7). A higher magnitude and rate of OVA release was observed at 37 °C in all instances. This difference is likely a consequence of the driving force created by the collapse of the PVCL network at 37 °C. The PVCL NGs presented the best protein retention at 25 °C and the strongest release at 37 °C. By contrast, difference in protein release by the hydrogels was less evident at the two respective temperatures. The patch presented an intermediate behaviour, where, although a notable amount of protein was released at 25 °C, considerably more exited the patch upon thermally triggered collapse at 37 °C. This variable behaviour could be a consequence of the location of the loaded protein within the investigated carrier systems.

Since the PVCL NGs were separated from unloaded protein, OVA will mainly be present inside their nano-PVCL matrices. In this scenario, the retention or exit of OVA

is mainly influenced by the volume changes that NGs experience with changing temperature. As previously described, OVA should be partitioned between the NGs structure and the interstitial voids of the PVCL/acrylic patches. Here, the OVA fraction loaded within the NG structures should be more susceptible to the temperature induced release triggered by the collapse of NGs structure. By comparison, the OVA fraction present in the interstitial spaces of the patch should be able to more easily exit the structure at 25 °C, in the presence of the swollen NG, as OVA does not have to diffuse through the crosslinked PVCL networks. Although unloaded OVA was separated from the loaded hydrogels, protein release was still important at 25 °C. This could be an indication that most of OVA was adsorbed onto the hydrogel surface, where a fast diffusion is independent of temperature media that induced structural changes to the hydrogel. This finding is in agreement with work published by Zhang and coworkers, in which the release of BSA from poly(*N*-isopropylacrylamide) hydrogels was investigated.[41]

CD spectra of OVA released from the three systems were recorded and compared to a free OVA solution (Figure 7.d). The secondary structure of the OVA remained intact following loading and release from all investigated systems, which is an indication that the structure of OVA was not affected. Therefore, it is expected that the therapeutic competence of loaded proteins can be maintained in a dermal application.

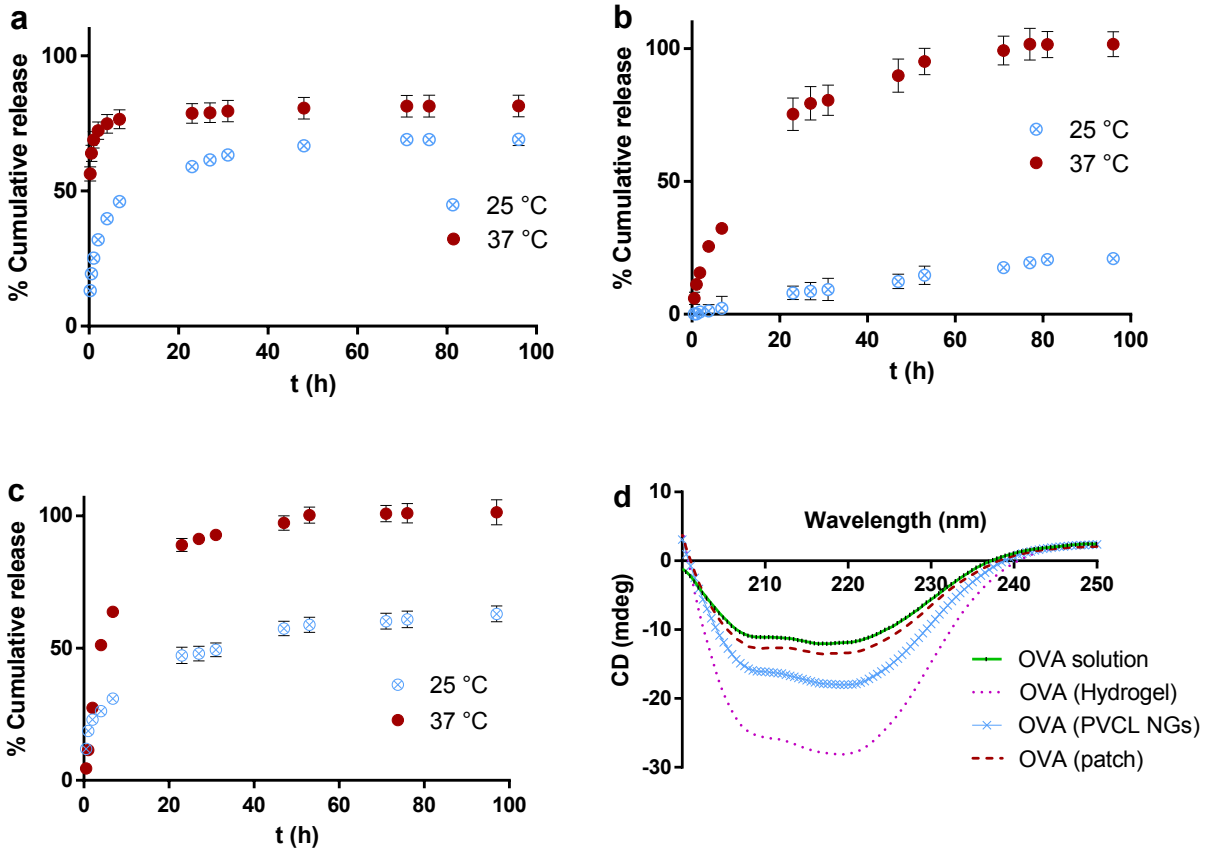

Figure 7. Ovalbumin release in PBS buffer from (a) hydrogel, (b) PVCL NGs, and (c) PVCL/acrylic patch. (d) Secondary structure of OVA released from the three systems and of a free OVA solution (n=3, mean ± SD).

Skin penetration of OVA delivered from the investigated carriers

Some extensively used methods to overcome the barrier of SC such as microneedles[42,43] and iontophoresis[44,45] are associated with various risks such as inflammation and infection due to acutely irreversible breakdown of the SC.[46] Taking the potential of the here investigated carriers into account, it is worth to compares their ability to act as dermal delivery systems. To be of use for topical immunization, the

investigated systems must be capable of delivering antigens past the SC into the viable epidermis of the skin. Therefore, the capability of these three carrier systems to facilitate OVA penetration into human skin was investigated. Skin biopsies, either intact or tape stripped – a common approach to mimic barrier deficient skin[47] – were topically treated with OVA in PBS or loaded within one of the three PVCL carriers, and exposed to a temperature ramp (30–37 °C) over a 6 h incubation period. Subsequently, OVA penetration was visualised. Figure 8 presents 2 images for each OVA penetration experiments. While left aligned images show OVA staining pseudocoloured with an intensity scale (shown at bottom of figure), right aligned images represent the overlays of OVA staining pseudocoloured red, nuclear staining pseudocoloured blue, and bright field in grey. Dashed yellow lines mark the dermal-epidermal boundary.

As expected, topical application of OVA dissolved in PBS resulted in little detectable penetration in both tape stripped and barrier intact skin (Figure 8.b). Application of the hydrogels resulted in very little protein delivery into intact skin (Figure 8.c). In tape-stripped skin, strong OVA staining was visible throughout the SC and some penetration into the viable epidermis was observed. By contrast, though again large amounts of OVA were seen throughout the SC of the tape stripped skin treated with OVA loaded PVCL NGs, notably more was visible within the viable epidermis (Figure 8.d). OVA staining of barrier intact skin was largely confined to the SC. These results are reminiscent of the topical protein delivery mediated by other thermoresponsive NGs.

For instance, NGs formed of dendritic polyglycerols by poly(*N*-isopropylacrylamide) or thermoresponsive polyglycerol have been shown to deliver proteins as large as 150 kDa past the SC of barrier deficient skin, in a manner apparently dependent on temperature triggered release and hydration induced disruptions to SC ordering. [21,24]

By contrast to the similarly structured hydrogels, the PVCL/acrylic patches produced more extensive staining within the SC of both the barrier intact and tape stripped skin, as well demonstrating apparent delivery of OVA to the viable epidermis of tape stripped skin comparable to the NGs (Figure 8.e). This difference could well correspond to stronger temperature dependent release of protein from the patches, as compared to the hydrogels (Figure 7), in addition to the occlusive nature of the patch topical application, a point previously shown to enhance skin hydration and subsequent macromolecule penetration.[30]

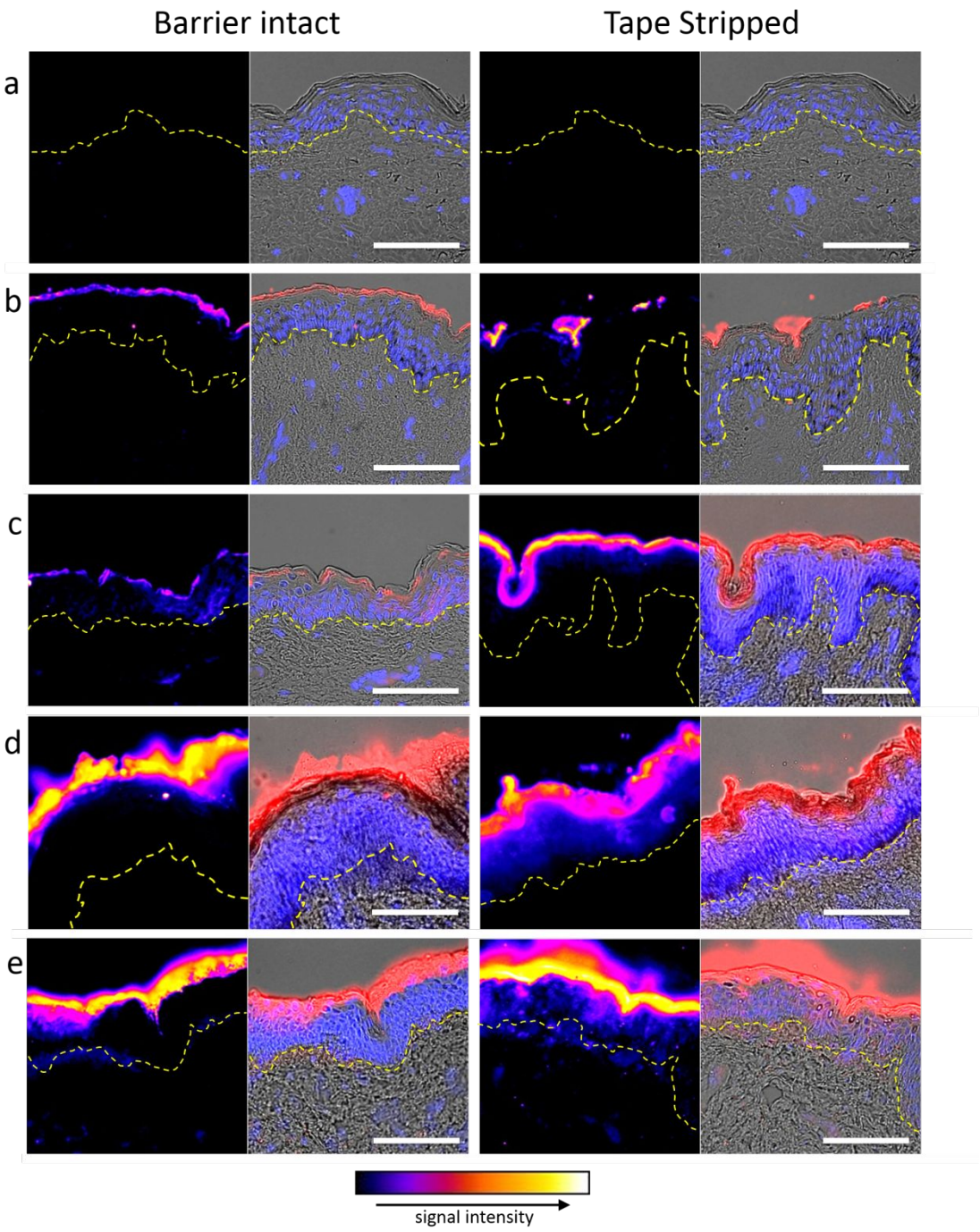

Figure 8. Representative ovalbumin immunohistochemistry (temperature map or red staining) of (a) untreated skin biopsies or skin biopsies treated with ovalbumin in (b) PBS, (c) hydrogels, (d) PVCL NGs, or (e) PVCL/acrylic patches. Dashed yellow lines

mark the dermal-epidermal boundary. Overlays show OVA staining (red), DAPI staining (blue), and bright field images (grey). Scale bars = 50 μm.

CONCLUSIONS

In this work we aimed to evaluate the effect varied structural compositions had on a delivery platforms ability to deliver antigens past the skin SC following topical application. For this, the biocompatible and thermoresponsive polymer PVCL was used to prepare three carriers that should enable the encapsulation of ovalbumin, and its subsequent temperature dependent release. The three structural variations consisted of a PVCL hydrogel with pore size in the range of 15-30 μm, PVCL NGs with an average collapsed diameter of 157 nm, and a nanostructured patch obtained by casting PVCL/acrylic NGs – average collapsed diameter 393 nm – with film formation capability. All three systems were able to load OVA, a model antigen, though the PVCL NGs showed the highest loading capacity. They also demonstrated a temperature triggered OVA release *in vitro*, where faster release rates were achieved when their media temperatures were raised above the carrier system's transition temperatures. The structural integrity of OVA was not affected by loading into, and release from the investigated systems. In comparison to application of OVA in PBS, which, as expected, resulted in negligible penetration, the OVA loaded carrier systems were more successful. The PVCL NGs only showed improved protein penetration in tape stripped skin, following the behavior of other reported thermosensitive NGs. Application of the

hydrogels resulted in little OVA penetration to the late epidermis of barrier intact and tape stripped skin. PVCL/acrylic patches appeared to achieve a greater amount of OVA delivery to the epidermis in both the barrier intact and tape stripped skin following topical application. The differences in the system's ability to deliver OVA to deeper layers of the skin could be related to their capability to shrink and expel the loaded protein upon sufficient thermal trigger, generating an additional penetration stimulus. These properties favour the NGs and nanostructured PVCL/acrylic patches, where the protein carriers are based on a nanoparticulate system. Considering the alteration of the SC caused by topical application of OVA loaded PVCL NGs, the PVCL/acrylic patch appears to be a good candidate as transdermal immunization system.

ACKNOWLEDGEMENTS

We gratefully acknowledge financial support from CONICET, ANPCyT, Universidad Nacional del Litoral, and Bundesministerium für Bildung und Forschung (BMBF, NanoMatFutur award 'ThermoNanogele', 13N12561). Ms. Ana Sonzogni acknowledges the DAAD for the financial support of her stay at the Freie Universität Berlin. Funding from the German Research Foundation (HE7440/2-1) to S.H. is gratefully acknowledged.

REFERENCES

(1) Richmond, J. M.; Harris, J. E. Immunology and Skin in Health and Disease. Cold Spring Harb. Perspect. Med. 2014, 4 (12), a015339–a015339.

(2) Babiuk, S.; Baca-Estrada, M.; Babiuk, L. A.; Ewen, C.; Foldvari, M. Cutaneous Vaccination: The Skin as an Immunologically Active Tissue and the Challenge of Antigen Delivery. J. Control. Release 2000, 66 (2–3), 199–214.

(3) Mitsui, H.; Watanabe, T.; Saeki, H.; Mori, K.; Fujita, H.; Tada, Y.; Asahina, A.; Nakamura, K.; Tamaki, K. Differential Expression and Function of Toll-like Receptors in Langerhans Cells: Comparison with Splenic Dendritic Cells. J. Invest. Dermatol. 2004, 122 (1), 95–102.

(4) Tay, S. S.; Roediger, B.; Tong, P. L.; Tikoo, S.; Weninger, W. The Skin-Resident Immune Network. Curr. Dermatol. Rep. 2014, 3 (1), 13–22.

(5) Choy, Y. Bin; Prausnitz, M. R. The Rule of Five for Non-Oral Routes of Drug Delivery: Ophthalmic, Inhalation and Transdermal. Pharm. Res. 2011, 28 (5), 943–948.

(6) Bouwstra, J. A.; Ponec, M. The Skin Barrier in Healthy and Diseased State. Biochim. Biophys. Acta - Biomembr. 2006, 1758 (12), 2080–2095.

(7) Glenn, G. M.; Taylor, D. N.; Li, X.; Frankel, S.; Montemarano, A.; Alving, C. R. Transcutaneous Immunization: A Human Vaccine Delivery Strategy Using a Patch. Nat. Med. 2000, 6 (12), 1403–1406.

(8) Shi, Z.; Curiel, D. T.; Tang, D. C. DNA-Based Non-Invasive Vaccination onto the Skin. Vaccine 1999, 17 (17), 2136–2141.

(9) Partidos, C. D.; Beignon, A.-S.; Mawas, F.; Belliard, G.; Briand, J.-P.; Muller, S. Immunity under the Skin: Potential Application for Topical Delivery of Vaccines. Vaccine 2003, 21 (7–8), 776–780.

(10) Mitragotri, S. Immunization without Needles. Nat. Rev. Immunol. 2005, 5 (12), 905–916.

(11) Hammond, S. A.; Guebre-Xabier, M.; Yu, J.; Glenn, G. M. Transcutaneous Immunization: An Emerging Route of Immunization and Potent Immunostimulation Strategy. Crit. Rev. Ther. Drug Carrier Syst. 2001, 18 (5), 503–526.

(12) Chen, Y.; Wu, Y.; Gao, J.; Zhang, Z.; Wang, L.; Chen, X.; Mi, J.; Yao, Y.; Guan, D.; Chen, B.; et al. Transdermal Vascular Endothelial Growth Factor Delivery with Surface Engineered Gold Nanoparticles. ACS Appl. Mater. Interfaces 2017, 9 (6), 5173–5180.

(13) Karande, P.; Jain, A.; Mitragotri, S. Insights into Synergistic Interactions in Binary Mixtures of Chemical Permeation Enhancers for Transdermal Drug Delivery. J. Control. Release 2006, 115 (1), 85–93.

(14) Chen, W.; Li, H.; Shi, D.; Liu, Z.; Yuan, W. Microneedles As a Delivery System for Gene Therapy. Front. Pharmacol. 2016, 7, 137.

(15) Chen, Y.; Shen, Y.; Guo, X.; Zhang, C.; Yang, W.; Ma, M.; Liu, S.; Zhang, M.; Wen, L.-P. Transdermal Protein Delivery by a Coadministered Peptide Identified via Phage Display. Nat. Biotechnol. 2006, 24 (4), 455–460.

(16) Vij, M.; Natarajan, P.; Pattnaik, B. R.; Alam, S.; Gupta, N.; Santhiya, D.; Sharma, R.; Singh, A.; Ansari, K. M.; Gokhale, R. S.; et al. Non-Invasive Topical Delivery of Plasmid DNA to the Skin Using a Peptide Carrier. J. Control. Release 2016, 222, 159–168.

(17) Gennari, C. G. M.; Franzè, S.; Pellegrino, S.; Corsini, E.; Vistoli, G.; Montanari, L.; Minghetti, P.; Cilurzo, F. Skin Penetrating Peptide as a Tool to Enhance the Permeation of Heparin through Human Epidermis. Biomacromolecules 2016, 17 (1), 46–55.

(18) Yang, Y.; Sunoqrot, S.; Stowell, C.; Ji, J.; Lee, C.-W.; Kim, J. W.; Khan, S. A.; Hong, S. Effect of Size, Surface Charge, and Hydrophobicity of Poly(amidoamine) Dendrimers on Their Skin Penetration. Biomacromolecules 2012, 13 (7), 2154–2162.

(19) Witting, M.; Boreham, A.; Brodwolf, R.; Vávrová, K.; Alexiev, U.; Friess, W.; Hedtrich, S. Interactions of Hyaluronic Acid with the Skin and Implications for the Dermal Delivery of Biomacromolecules. Mol. Pharm. 2015, 12 (5), 1391–1401.

(20) Matsuo, K.; Ishii, Y.; Quan, Y. S.; Kamiyama, F.; Mukai, Y.; Yoshioka, Y.; Okada, N.; Nakagawa, S. Transcutaneous Vaccination Using a Hydrogel Patch Induces Effective Immune Responses to Tetanus and Diphtheria Toxoid in Hairless Rat. J. Control. Release 2011, 149 (1), 15–20.

(21) Witting, M.; Molina, M.; Obst, K.; Plank, R.; Eckl, K. M.; Hennies, H. C.; Calderón, M.; Frieβ, W.; Hedtrich, S. Thermosensitive Dendritic Polyglycerol-Based Nanogels for Cutaneous Delivery of Biomacromolecules. Nanomedicine Nanotechnology, Biol. Med. 2015, 11 (5), 1179–1187.

(22) Edlich, A.; Gerecke, C.; Giulbudagian, M.; Neumann, F.; Hedtrich, S.; Schäfer-Korting, M.; Ma, N.; Calderon, M.; Kleuser, B. Specific Uptake Mechanisms of Well-Tolerated Thermoresponsive Polyglycerol-Based Nanogels in Antigen-Presenting Cells of the Skin. Eur. J. Pharm. Biopharm. 2016, 116, 155–163.

(23) Giulbudagian, M.; Rancan, F.; Klossek, A.; Yamamoto, K.; Jurisch, J.; Neto, V. C.; Schrade, P.; Bachmann, S.; Rühl, E.; Blume-Peytavi, U.; et al. Correlation between the Chemical Composition of Thermoresponsive Nanogels and Their Interaction with the Skin Barrier. J. Control. Release 2016, 243, 323–332.

(24) Giulbudagian, M.; Yealland, G.; Hönzke, S.; Edlich, A.; Geisendörfer, B.; Kleuser, B.; Hedtrich, S.; Calderón, M. Breaking the Barrier – Potent Anti-Inflammatory Activity Following Efficient Topical Delivery of Etanercept Using Thermoresponsive Nanogels. Theranostics 2018, 8 (2), 450–463.

(25) Sonzogni, A. S.; Passeggi, M. C. G.; Wedepohl, S.; Calderón, M.; Gugliotta, L. M.; Gonzalez, V. D. G.; Minari, R. J. Thermoresponsive Nanogels with Film-Forming Ability. Polym. Chem. 2018, 9, 1004–1011.

(26) Vihola, H.; Laukkanen, A.; Valtola, L.; Tenhu, H.; Hirvonen, J. Cytotoxicity of Thermosensitive Polymers poly(N-Isopropylacrylamide), poly(N-Vinylcaprolactam) and Amphiphilically Modified poly(N-Vinylcaprolactam). Biomaterials 2005, 26 (16), 3055–3064.

(27) Gao, Y.; Au-Yeung, S. C. F.; Wu, C. Interaction between Surfactant and Poly(N-Vinylcaprolactam) Microgels. Macromolecules 1999, 32 (11), 3674–3677.

(28) Bradford, M. M. A Rapid and Sensitive Method for the Quantitation of Microgram Quantities of Protein Utilizing the Principle of Protein-Dye Binding. Anal. Biochem. 1976, 72 (1–2), 248–254.

(29) Schindelin, J.; Arganda-Carreras, I.; Frise, E.; Kaynig, V.; Longair, M.; Pietzsch, T.; Preibisch, S.; Rueden, C.; Saalfeld, S.; Schmid, B.; et al. Fiji: An Open-Source Platform for Biological-Image Analysis. Nat. Methods 2012, 9 (7), 676–682.

(30) Benson, H. A. E. Transdermal Drug Delivery: Penetration Enhancement Techniques. Curr. Drug Deliv. 2005, 2 (1), 23–33.

(31) Bergueiro, J.; Calderón, M. Thermoresponsive Nanodevices in Biomedical Applications. Macromol. Biosci. 2015, 15 (2), 183–199.

(32) Meeussen, F. Phase Behaviour of poly(N-Vinyl Caprolactam) in Water. Polymer (Guildf). 2000, 41 (24), 8597–8602.

(33) Solomon, O. F.; Corciovei, M.; Ciută, I.; Boghină, C. Properties of Solutions of poly-N-vinylcaprolactam. 1968, 12 (8), 1835–1842.

(34) Makhaeva, E. E.; Thanh, L. T. M.; Starodoubtsev, S. C.; Khokhlov, A. R. Thermoshrinking Behavior of Poly(vinylcaprolactam) Gels in Aqueous Solution. 1996, 197 (6), 1973–1982.

(35) Cortez-Lemus, N. A.; Licea-Claverie, A. Poly(N-Vinylcaprolactam), a Comprehensive Review on a Thermoresponsive Polymer Becoming Popular. Prog. Polym. Sci. 2016, 53, 1–51.

(36) Imaz, A.; Forcada, J. N -Vinylcaprolactam-Based Microgels: Synthesis and Characterization. J. Polym. Sci. Part A Polym. Chem. 2008, 46 (7), 2510–2524.

(37) Behl, C. R.; Flynn, G. L.; Kurihara, T.; Harper, N.; Smith, W.; Higuchi, W. I.; Ho, N. F.; Pierson, C. L. Hydration and Percutaneous Absorption: I. Influence of Hydration on Alkanol Permeation through Hairless Mouse Skin. J. Invest. Dermatol. 1980, 75 (4), 346–352.

(38) McKENZIE, A.; STOUGHTON, R. Method for Comparing Percutaneous Absorption of Steroids. Arch. Dermatol 1962, 86, 608–610.

(39) Benedict, F. G.; Miles, W. R.; Johnson, A. The Temperature of the Human Skin. Proc. Natl. Acad. Sci. USA 1919, 5 (6), 218–222.

(40) Fröhlich, E. The Role of Surface Charge in Cellular Uptake and Cytotoxicity of Medical Nanoparticles. Int. J. Nanomedicine 2012, 7, 5577–5591.

(41) Zhang, X.-Z.; Wu, D.-Q.; Chu, C.-C. Synthesis, Characterization and Controlled Drug Release of Thermosensitive IPN–PNIPAAm Hydrogels. Biomaterials 2004, 25, 3793–3805.

(42) Henry, S.; McAllister, D. V; Allen, M. G.; Prausnitz, M. R. Microfabricated Microneedles: A Novel Approach to Transdermal Drug Delivery. J. Pharm. Sci. 1998, 87 (8), 922–925.

(43) Arya, J.; Prausnitz, M. R. Microneedle Patches for Vaccination in Developing Countries. J. Control. Release 2016, 240, 135–141.

(44) Priya, B.; Rashmi, T.; Bozena, M.; Rashmi, T.; Michniak, B.; Bozena, M. Transdermal Iontophoresis. Expert Opin. Drug Deliv. 2006, 3 (1), 127–138.

(45) Wang, Y.; Thakur, R.; Fan, Q.; Michniak, B. Transdermal Iontophoresis: Combination Strategies to Improve Transdermal Iontophoretic Drug Delivery. Eur. J. Pharm. Biopharm. 2005, 60 (2), 179–191.

(46) Ishii, Y.; Nakae, T.; Sakamoto, F.; Matsuo, K.; Matsuo, K.; Quan, Y. S.; Kamiyama, F.; Fujita, T.; Yamamoto, A.; Nakagawa, S.; et al. A Transcutaneous Vaccination System Using a Hydrogel Patch for Viral and Bacterial Infection. J. Control. Release 2008, 131 (2), 113–120.

(47) Bashir, S. J.; Chew, A. L.; Anigbogu, A.; Dreher, F.; Maibach, H. I. Physical and Physiological Effects of Stratum Corneum Tape Stripping. Skin Res. Technol. 2001, 7 (1), 40–48.

For Table of Contents Only

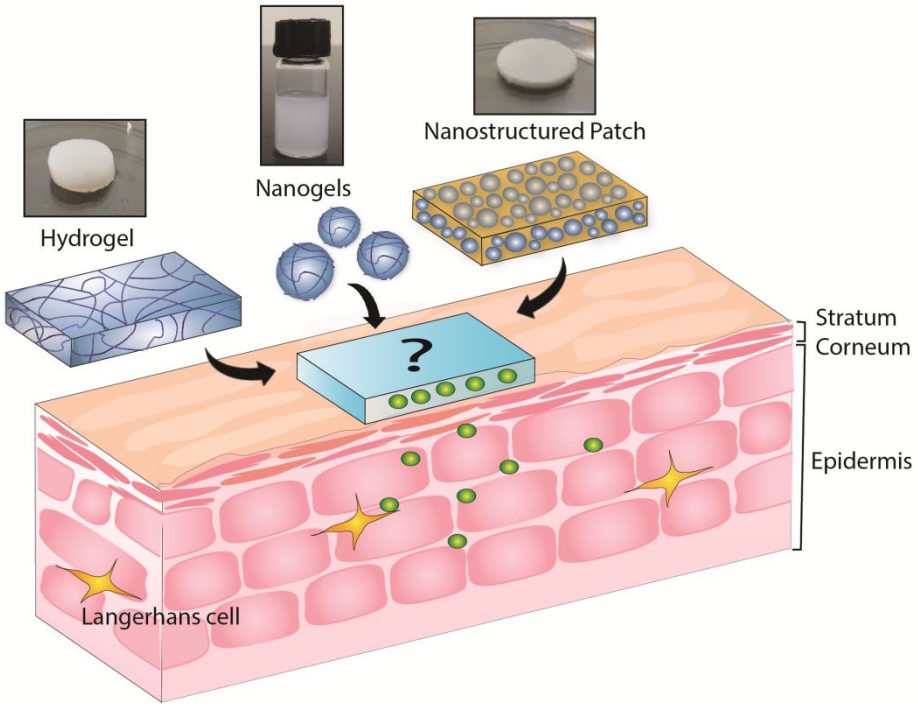

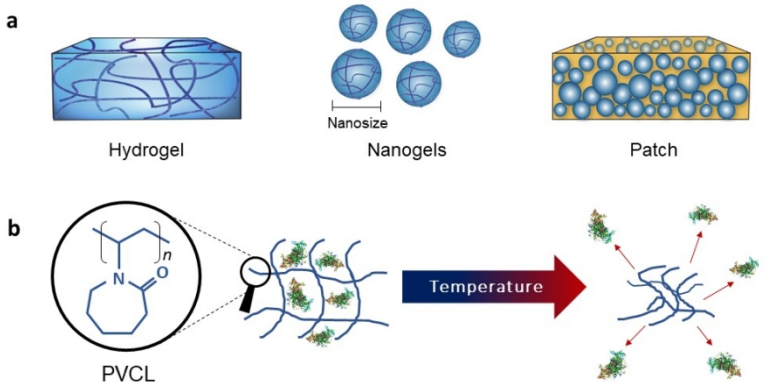

Figure 1. Scheme of (a) the three investigated systems and of (b) the thermoresponsive character of PVCL (b).

338x190mm (96 x 96 DPI)

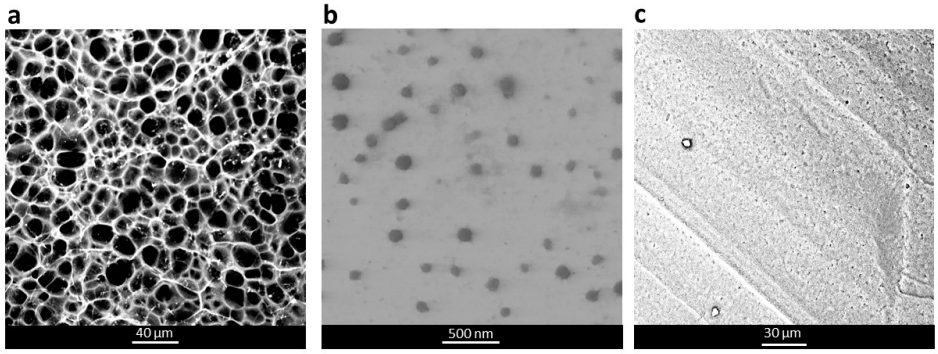

Figure 2. Microscopy images of the studied carrier platforms: (a) hydrogel, (b) PVCL NGs and (c) PVCL/acrylic patch.

338x190mm (96 x 96 DPI)

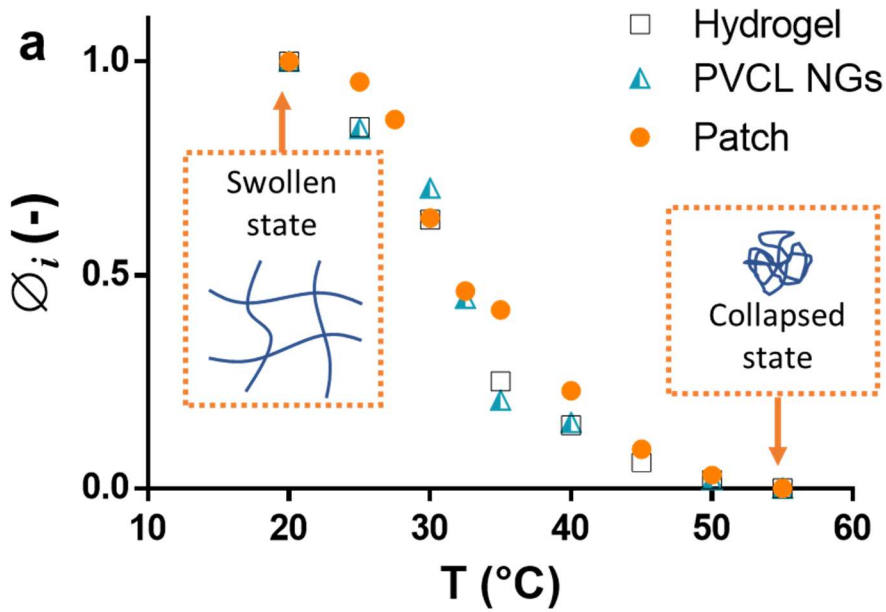
a
1.0
0.5
0.0
$\varnothing_i$ (-)
10
20
30
40
50
60
T (°C)
Hydrogel
PVCL NGs
Patch
Swollen state
Collapsed state

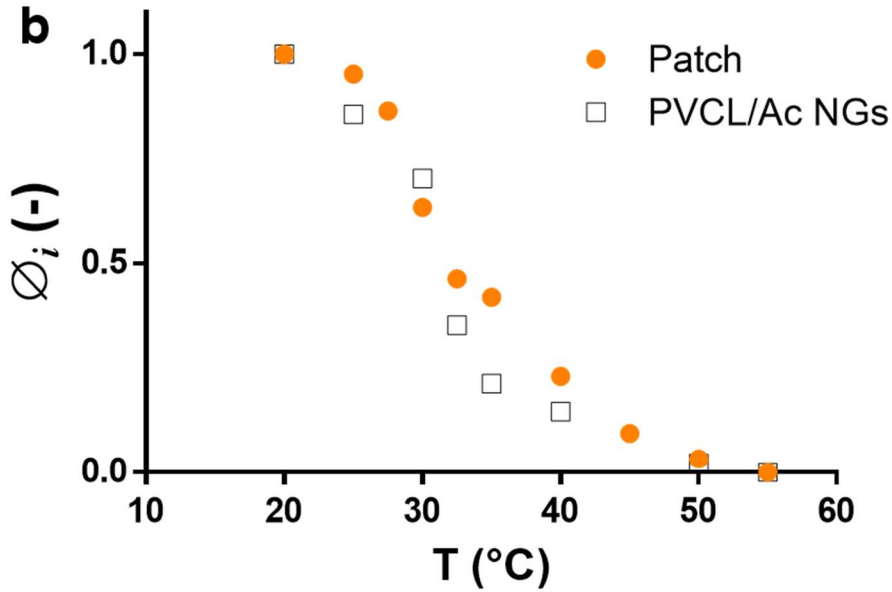
b
1.0
0.5
0.0
$\varnothing_i$ (-)
10
20
30
40
50
60
T (°C)
Patch
PVCL/Ac NGs

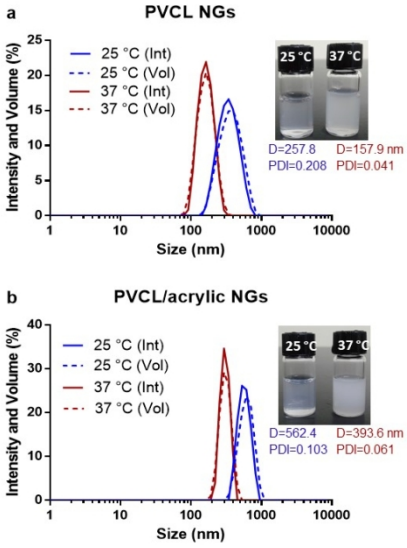

Figure 4. DLS intensity and volume distributions at 25 and 37 °C of (a) PVCL NGs and (b) PVCL/acrylic NGs.

338x190mm (96 x 96 DPI)

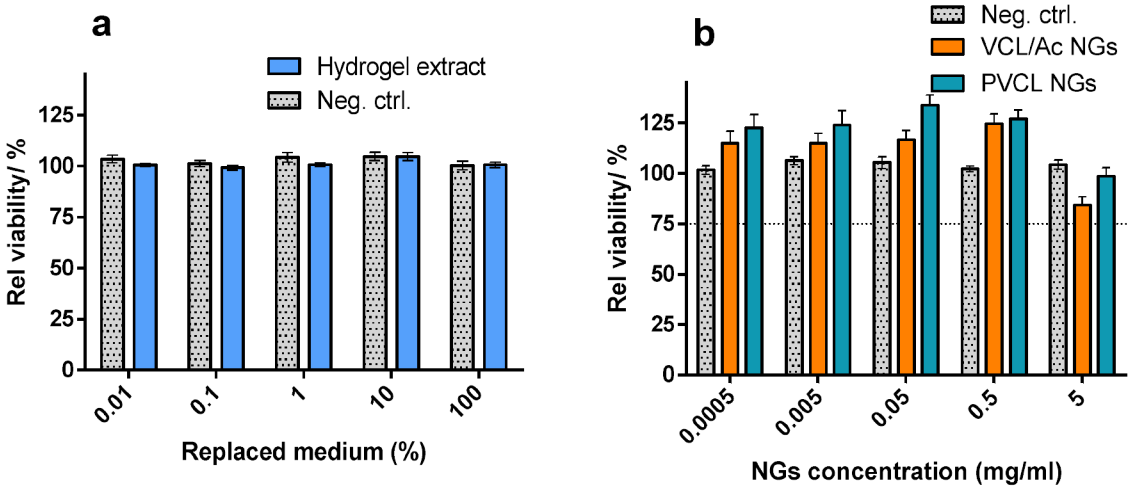
a
Hydrogel extract
Neg. ctrl.
Rel viability/ %
125
100
75
50
25
0
0.01
0.1
1
10
100
Replaced medium (%)
b
Neg. ctrl.
VCL/Ac NGs
PVCL NGs
Rel viability/ %
125
100
75
50
25
0
0.0005
0.005
0.05
0.5
5
NGs concentration (mg/ml)

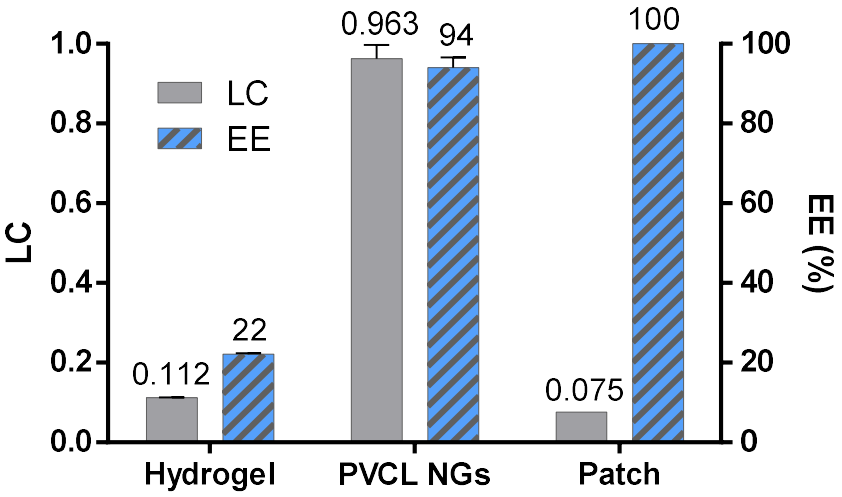
LC
EE
0.963
94
100
0.112
22
0.075
1.0
0.8
0.6
0.4
0.2
0.0
100
80
60
40
20
0
LC
EE (%)
Hydrogel
PVCL NGs
Patch

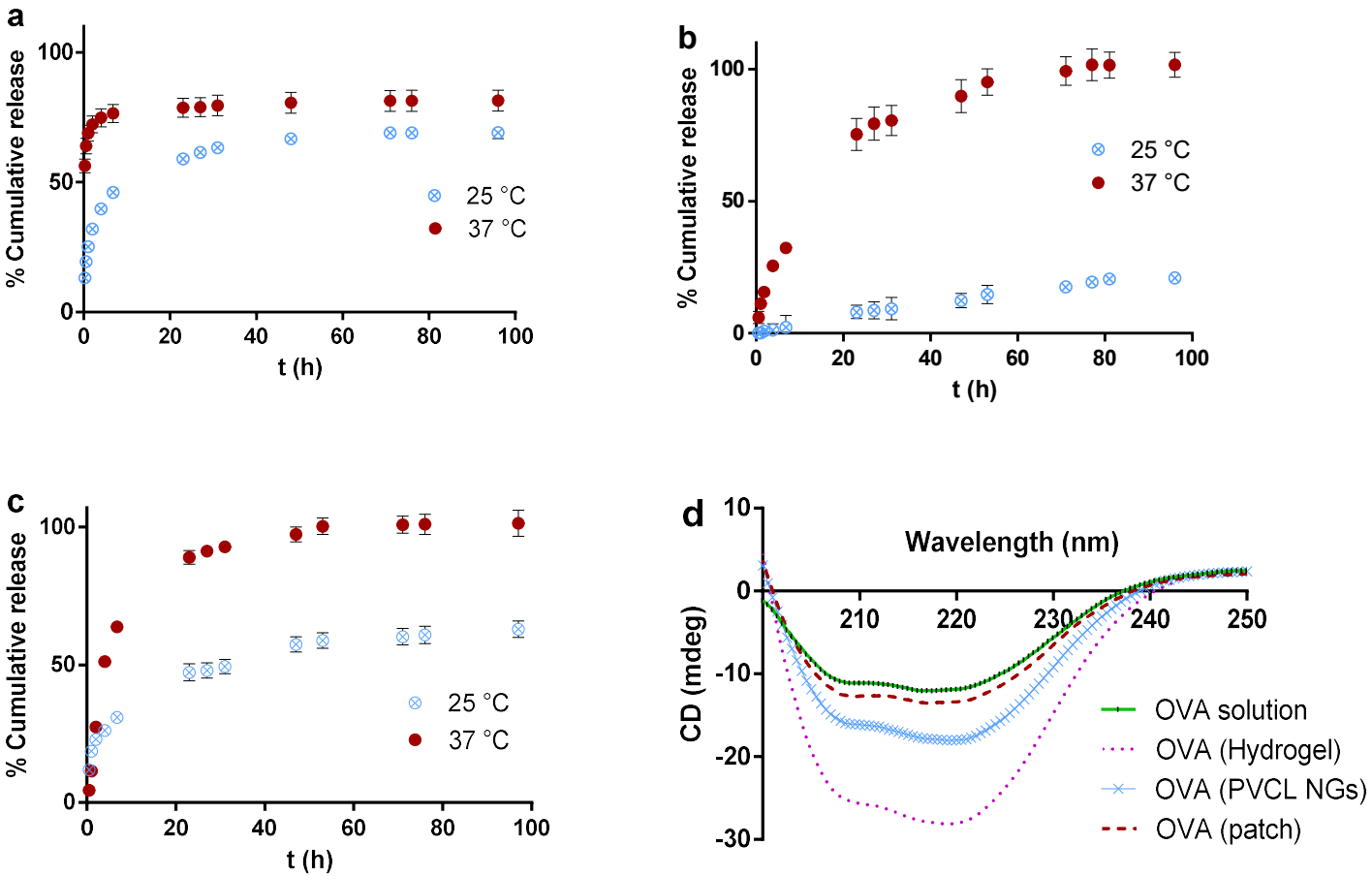
a
% Cumulative release
t (h)
25 °C
37 °C
b
% Cumulative release
t (h)
25 °C
37 °C
c
% Cumulative release
t (h)
25 °C
37 °C
d
Wavelength (nm)
CD (mdeg)
OVA solution
OVA (Hydrogel)
OVA (PVCL NGs)
OVA (patch)

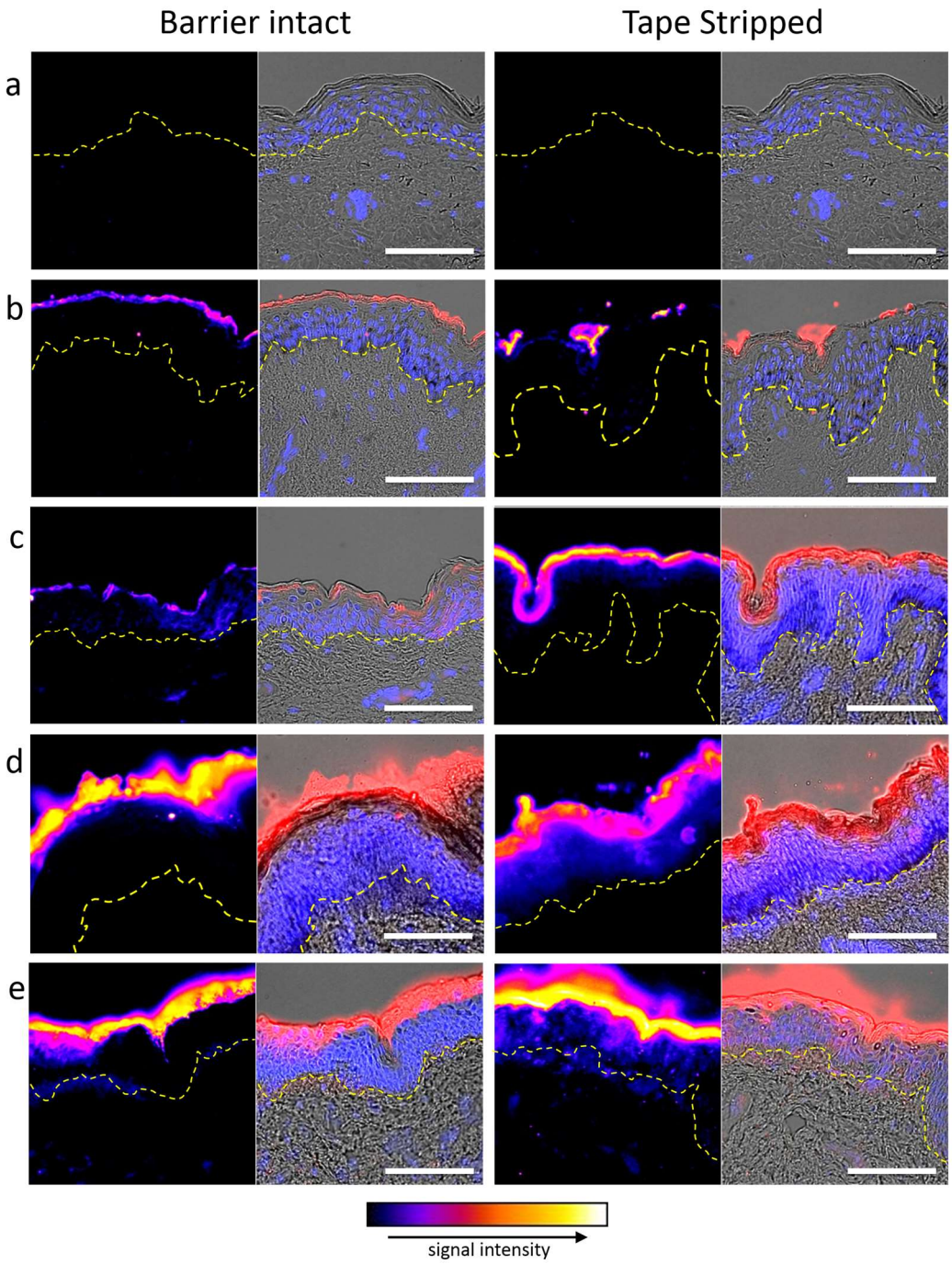
Barrier intact
Tape Stripped
a
b
c
d
e
signal intensity

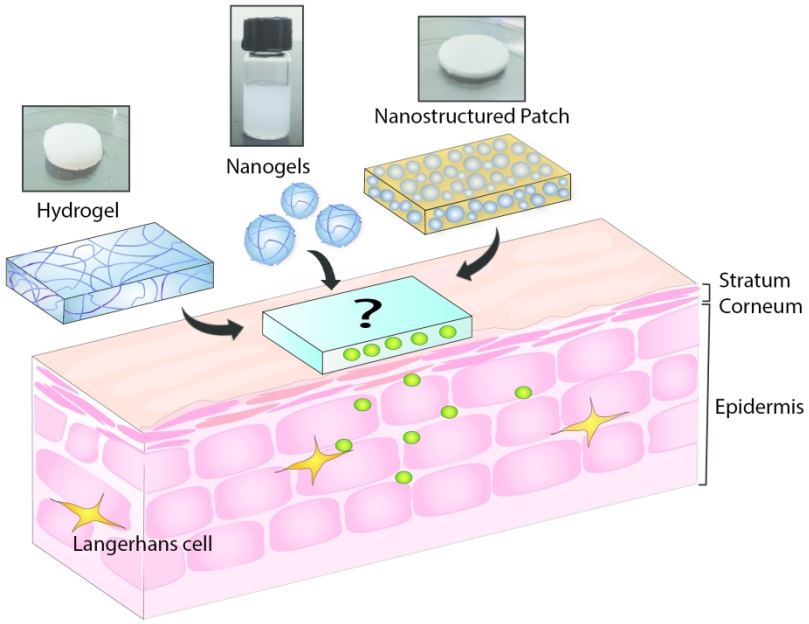

For Table of Content Only

229x154mm (300 x 300 DPI)